

G^2 Blending of Cubic Pythagorean Hodograph Curves with Prescribed Total Arc Length

Yongxia HAO*, Lianxing LIAO

School of Mathematical Sciences, Jiangsu University, Jiangsu 212000, P. R. China

Abstract Pythagorean-hodograph (PH) curve is widely used in curve modeling because of its advantages in arc length and equidistant curve calculation. This paper discusses the G^2 continuous blending of cubic PH curves under total arc length constraint. Given three points including two end control points and a joint point, construct two cubic PH curves such that they interpolate the end control points and are G^2 continuous at joint point with prescribed total arc length. It can also be regarded as a curve extension problem. According to the arc length formula of cubic PH curve and the condition of G^2 blending, the problem is transformed into a constrained minimization problem. Several examples are served to illustrate our method.

Keywords Pythagorean-hodograph curve; G^2 blending; prescribed arc length; nonlinear equations

MR(2020) Subject Classification 65D17; 68U07

1. Introduction

Pythagorean-hodograph (PH) curves, introduced by Farouki and Sakkalis in 1990 (see [1]), have been extensively studied in the past few decades. Because of their unique properties, such as exact representation of polynomial arc length and rational offset, they are widely used in geometric modeling and CNC machining [2]. We refer the reader to the book [3] for theories and techniques about PH curves as well as their applications in CAGD, or a recent survey paper [4].

A lot of work have been given in the literature to deal with the problem of interpolating the boundary data, such as curve blending, curve interpolation and curve extension. Geometric continuity is often required in these operations. According to the advantages of PH curve, a PH curve may also have a prescribed arc length besides interpolating the boundary data. Farouki [5] proposed a problem of interpolating planar G^1 Hermite data under arc length constraint and developed a closed-form solution using quintic PH curves. A generalization of the results from planar to spatial quintic PH curves was studied in [6]. Huard et al. [7] defined a spatial C^2 PH quintic spline interpolating a sequence of nodal points with specified internodal arc length, by solving a system of nonlinear equations. Krajnc [8] studied the problem of interpolating spatial G^1 data using rational PH curves with prescribed arc length and provided a closed-form solution.

Received July 13, 2020; Accepted November 15, 2020

Supported by the National Natural Science Foundation of China (Grant No. 11801225), University Science Research Project of Jiangsu Province (Grant No. 18KJB110005) and the Research Foundation for Advanced Talents of Jiangsu University (Grant No. 14JDG034).

* Corresponding author

E-mail address: yongxiahaoujs@ujs.edu.cn (Yongxia HAO)

In parametric curve design, a complicated curve sometimes can not have a unified expression, so the curve usually is expressed by dividing into several poly-segment curves. A practical and straightforward method is extending or blending based on geometric continuity and energy constraints. Using single or multi-connected PH curves to approximate general smooth curves or fit discrete data or interpolate Hermite data is an efficient way, which has been used in various applications [9–11]. This paper also makes use of the property that the arc length of PH curve can be expressed in an accurate polynomial formula, and focuses on the study of a pair of G^2 blending cubic PH curves with prescribed total arc length. The G^2 continuity of parametric curve segments adopted here means that the position, tangent and curvature of the two adjacent segments are continuous at the junction [12]. Specifically, given two distinct points and another point as joint point, two interpolating cubic PH curves with G^2 continuity at the joint point and prescribed total length are constructed. The free parameters of the PH curves are then obtained by solving a constrained minimization problem developed from the interpolation conditions of end points and the constraint of a specified total arc length.

There are other two kinds of applications of our work. The first application deals with the reconstruction of physical surfaces by means of a ribbon device (the Morphosense ribbon) equipped with micro-sensors [13], just like the work in [7, 14]; The second application is that our work can be regarded as a special case of curve extension which is an important operation in computer aided design system. Given an original curve $P(t)$ and several target points $\{R_i\}$, curve extension methods aim to find a resulting curve $R(t)$, which contains all the curve points of $P(t)$ and also passes through every target point R_i . Our work can be considered as a special case of curve extension problem in that only the two end points of the original curve $P(t)$ are known.

The remainder of this paper is organized as follows. Some preliminaries and commonly used properties of PH curves are introduced in Section 2. Section 3 describes the problem and the technique of G^2 blending by two planar cubic PH curves with prescribed total arc length. Section 4 illustrates our method by proposing several examples. Finally, we conclude in Section 5 with a brief summary and discussion.

2. Planar Pythagorean-hodograph curves

The definition of PH curve and its related theorems and corollaries are as follows.

Theorem 2.1 ([1]) *A Pythagorean-hodograph curve $P(t) = (x(t), y(t))$, $t \in [0, 1]$ has derivative components $x'(t)$, $y'(t)$ satisfying the condition*

$$x'^2(t) + y'^2(t) = \sigma^2(t)$$

for some polynomial $\sigma(t)$.

$\sigma(t)$ specifies the parametric speed of $P(t)$, i.e., the derivative of the arc length s with respect

to the curve parameter t , then the cumulative arc length function is

$$s(t) = \int_0^t \sigma(\xi) d\xi.$$

This feature makes PH curves have a lot of attractive computational properties: their arc lengths are exactly computable as polynomials; their normals and curvatures, offset curves and unit tangents are accurate rational polynomials; they are very suitable for real-time precision motion control applications [5].

A planar Bézier curve $r(t)$, $t \in [0, 1]$ with control points $\{P_i\}_{i=0}^n$ can be expressed as

$$r(t) = \sum_{i=0}^n P_i B_i^n(t)$$

where $B_i^n(t)$ is Bernstein basis function, and its hodograph curve is

$$r'(t) = n \sum_{i=0}^{n-1} \Delta P_i B_i^{n-1}(t), \quad \Delta P_i = P_{i+1} - P_i.$$

Theorem 2.2 ([1]) *The cubic Bézier curve $r(t) = \sum_{i=0}^3 P_i B_i^3(t)$ is a PH curve if and only if its control points $\{P_i\}_{i=0}^3$ satisfy the following relations:*

$$\begin{cases} P_1 = P_0 + \frac{1}{3}(u_0^2 - v_0^2, 2u_0v_0), \\ P_2 = P_1 + \frac{1}{3}(u_0u_1 - v_0v_1, u_0v_1 + u_1v_0), \\ P_3 = P_2 + \frac{1}{3}(u_1^2 - v_1^2, 2u_1v_1), \end{cases}$$

where u_0, v_0, u_1 and v_1 are real numbers, P_0 is a free initial control point.

Corollary 2.3 *The arc length of cubic PH curve $r(t) = \sum_{i=0}^3 P_i B_i^3(t)$ with control points in Theorem 2.1 can be expressed as:*

$$S = s(1) = \frac{1}{3}(u_0^2 + v_0^2 + u_0u_1 + v_0v_1 + u_1^2 + v_1^2).$$

Theorem 2.4 ([12]) *Suppose that the control points of two cubic PH curves $L(t)$ and $R(t)$ are P_0, P_1, P_2, P_3 and Q_0, Q_1, Q_2, Q_3 respectively, then these two curves are G^2 continuous at common point P_3 (Q_0) if the control points satisfy the following relations:*

$$\begin{cases} Q_0 = P_3, \\ Q_1 = P_3 + \alpha(P_3 - P_2), \\ Q_2 = P_3 + \alpha(P_3 - P_2) - \alpha^2(P_2 - P_1) + \gamma(P_3 - P_2), \end{cases}$$

where $\alpha > 0, \gamma$ are real numbers.

3. G^2 blending with prescribed total arc length

In this section, we present the specific problem and show a detailed discussion and analysis.

3.1. Description of the problem

Given three points

$$P_0 = (x_0, y_0), P_3 = Q_0 = (x_3, y_3), Q_3 = (x_4, y_4),$$

construct two cubic PH Bézier curves $L(t)$ and $R(t)$ as follows:

$$L(t) = \sum_{i=0}^3 P_i B_i^3(t), R(t) = \sum_{i=0}^3 Q_i B_i^3(t), \quad t \in [0, 1]$$

where all the inner control points P_1, P_2, Q_1, Q_2 are unknown. G^2 blending of these two curves is required at the joint point $P_3(Q_0)$ of the two curves and the total arc length $l = S_L + S_R$ is prescribed. By the profound analyses on existence of PH interpolants with specified end points, tangent data and a desired total arc length in [5, 6], we can conclude that the above problem is solvable.

Obviously, according to Theorem 2.2 and Corollary 2.3, we have the following relations about the control points $\{P_i\}_{i=0}^3$ and $\{Q_i\}_{i=0}^3$:

$$\begin{cases} P_1 = P_0 + \frac{1}{3}(u_0^2 - v_0^2, 2u_0v_0), \\ P_2 = P_1 + \frac{1}{3}(u_0u_1 - v_0v_1, u_0v_1 + u_1v_0), \\ P_3 = P_2 + \frac{1}{3}(u_1^2 - v_1^2, 2u_1v_1), \\ Q_1 = Q_0 + \frac{1}{3}(s_0^2 - t_0^2, 2s_0t_0), \\ Q_2 = Q_1 + \frac{1}{3}(s_0s_1 - t_0t_1, s_0t_1 + s_1t_0), \\ Q_3 = Q_2 + \frac{1}{3}(s_1^2 - t_1^2, 2s_1t_1), \end{cases} \quad (3.1)$$

where $u_0, v_0, u_1, v_1, s_0, t_0, s_1, t_1$ are all real numbers, and the total arc length of the two curves is

$$\begin{aligned} S &= S_L + S_R \\ &= \frac{1}{3}(u_0^2 + v_0^2 + u_0u_1 + v_0v_1 + u_1^2 + v_1^2 + s_0^2 + t_0^2 + s_0s_1 + t_0t_1 + s_1^2 + t_1^2) \\ &= l. \end{aligned} \quad (3.2)$$

Considering that $L(t)$ and $R(t)$ are G^2 blending at common point $P_3(Q_0)$ and combining Theorem 2.4, we have

$$\begin{cases} P_3 + \alpha(P_3 - P_2) - Q_1 = 0, \\ P_3 + \alpha(P_3 - P_2) - \alpha^2(P_2 - P_1) + \gamma(P_3 - P_2) - Q_2 = 0, \end{cases} \quad (3.3)$$

where $\alpha > 0, \gamma$ are real numbers. Therefore, the problem is transformed into solving the inner control points P_1, P_2, Q_1, Q_2 under the constraints (3.1)–(3.3), then we can obtain two G^2 blending curves $L(t)$ and $R(t)$ with prescribed total arc length l .

Remark 3.1 Obviously, there is no solution if $l < d$, and a trivial straight-line solution if $l = d$, where d refers to the distance between $P_0, P_3(Q_0)$ and Q_3 , i.e., $d = |P_3 - P_0| + |Q_3 - Q_0|$.

3.2. Analysis of constraints

Substituting $P_0 = (x_0, y_0), Q_0 = (x_3, y_3)$ into Eq. (3.1), we can express the control points $P_1, P_2, P_3, Q_1, Q_2, Q_3$ by x_0, y_0, x_3, y_3 . Then by Eqs. (3.2) and (3.3), we have the following result.

Proposition 3.2 *The two cubic PH Bézier curves $L(t), R(t)$ with G^2 continuity at joint point*

$P_3 = Q_0$ and the specified total arc length l satisfy the following system of equations:

$$\begin{cases} P_3 - (x_3, y_3) = 0, \\ Q_3 - (x_4, y_4) = 0, \\ P_3 + \alpha(P_3 - P_2) - Q_1 = 0, \\ P_3 + \alpha(P_3 - P_2) - \alpha^2(P_2 - P_1) + \gamma(P_3 - P_2) - Q_2 = 0, \\ u_0^2 + v_0^2 + u_0u_1 + v_0v_1 + u_1^2 + v_1^2 + s_0^2 + t_0^2 + s_0s_1 + t_0t_1 + s_1^2 + t_1^2 = 3l, \end{cases} \tag{3.4}$$

where $\alpha > 0, \gamma, u_0, v_0, u_1, v_1, s_0, t_0, s_1, t_1$ are all real numbers.

Remark 3.3 Since there are two components in every control point, the system (3.4) actually defines 9 equations with 10 parameters $u_0, u_1, v_0, v_1, s_0, s_1, t_0, t_1, \alpha, \gamma$, therefore the solution is not unique.

Expanding the equations in system (3.4), we can get the following specific expressions.

Theorem 3.4 The equations in Proposition 3.2 can be expressed by the following equations:

$$\begin{cases} \alpha u_1 v_1 - s_0 t_0 = 0, \\ \alpha(u_1^2 - v_1^2) - s_0^2 + t_0^2 = 0, \\ u_0^2 + u_0u_1 + u_1^2 - v_0^2 - v_0v_1 - v_1^2 + 3x_0 - 3x_3 = 0, \\ 2(u_0v_0 + u_1v_1) + u_0v_1 + u_1v_0 + 3y_0 - 3y_3 = 0, \\ s_0^2 + s_0s_1 + s_1^2 - t_0^2 - t_0t_1 - t_1^2 + 3x_3 - 3x_4 = 0, \\ 2(s_0t_0 + s_1t_1) + s_0t_1 + s_1t_0 + 3y_3 - 3y_4 = 0, \\ (\alpha + \gamma)(u_1^2 - v_1^2) - \alpha^2(u_0u_1 - v_0v_1) - s_0^2 + t_0^2 - s_0s_1 + t_0t_1 = 0, \\ 2(\alpha + \gamma)(u_1v_1) - \alpha^2(u_0v_1 + u_1v_0) - 2s_0t_0 - s_0t_1 - s_1t_0 = 0, \\ u_0^2 + v_0^2 + u_0u_1 + v_0v_1 + u_1^2 + v_1^2 + s_0^2 + t_0^2 + s_0s_1 + t_0t_1 + s_1^2 + t_1^2 = 3l, \end{cases} \tag{3.5}$$

where $\alpha > 0, \gamma, u_0, v_0, u_1, v_1, s_0, t_0, s_1, t_1$ are all real numbers.

Obviously, the system (3.5) is nonlinear equations. When the size of nonlinear equations is not too large, Newton methods and Gauss-Newton methods are efficient [15], but they need to compute the Jacobian matrix. It is well-known that the classical Newton method possesses quadratic convergence rate. Quasi-Newton methods are also popular since they have locally superlinear convergence and need not computing the Jacobian [16].

3.3. Analysis by complex representation

In this section, the complex representation will be adopted here to analyze the above problem. A PH curve $r(t)$ of degree $n = 2m + 1$ is generated from a degree m complex polynomial

$$h(t) = u(t) + iv(t) = \sum_{k=0}^m \mathbf{w}_k B_k^m(t)$$

with Bernstein coefficients $\mathbf{w}_k = u_k + iv_k, k = 0, 1$ by integration of the expression

$$r'(t) = h^2(t).$$

The parametric speed $\sigma(t)$ and the cumulative arc length function $s(t)$ are

$$\sigma(t) = |h(t)|^2, \quad s(t) = \int_0^t \sigma(\xi) d\xi.$$

A planar PH cubic is obtained by choosing $m = 1$. Suppose the cubic PH curve $L(t)$ and $R(t)$ are generated from the following two complex polynomials:

$$w(t) = u(t) + iv(t) = \mathbf{w}_0(1 - t) + \mathbf{w}_1t, \quad v(t) = u(t) + iv(t) = \mathbf{v}_0(1 - t) + \mathbf{v}_1t$$

respectively. On integrating, the Bézier control points P_k, Q_k of the resulting PH cubic

$$L(t) = \sum_{k=0}^3 P_k B_k^3(t), \quad R(t) = \sum_{k=0}^3 Q_k B_k^3(t)$$

can be expressed as

$$\begin{cases} P_1 = P_0 + \frac{1}{3}\mathbf{w}_0^2, \\ P_2 = P_1 + \frac{1}{3}\mathbf{w}_0\mathbf{w}_1, \\ P_3 = P_2 + \frac{1}{3}\mathbf{w}_1^2, \\ Q_1 = Q_0 + \frac{1}{3}\mathbf{v}_0^2, \\ Q_2 = Q_1 + \frac{1}{3}\mathbf{v}_0\mathbf{v}_1, \\ Q_3 = Q_2 + \frac{1}{3}\mathbf{v}_1^2. \end{cases}$$

By this complex expression, the conditions of G^2 continuity and the end points interpolation turn into

$$\begin{cases} \mathbf{v}_0^2 = \alpha\mathbf{w}_1^2, \\ \mathbf{v}_0\mathbf{v}_1 = \gamma\mathbf{w}_1^2 - \alpha^2\mathbf{w}_0\mathbf{w}_1, \end{cases} \tag{3.6}$$

and

$$\begin{cases} \mathbf{w}_0^2 + \mathbf{w}_0\mathbf{w}_1 + \mathbf{w}_1^2 = 3(P_3 - P_0), \\ \mathbf{v}_0^2 + \mathbf{v}_0\mathbf{v}_1 + \mathbf{v}_1^2 = 3(Q_3 - P_3), \end{cases} \tag{3.7}$$

respectively, while their total arc length is

$$l = \frac{|\mathbf{w}_0|^2 + \operatorname{Re}(\overline{\mathbf{w}_0}\mathbf{w}_1) + |\mathbf{w}_1|^2}{3} + \frac{|\mathbf{v}_0|^2 + \operatorname{Re}(\overline{\mathbf{v}_0}\mathbf{v}_1) + |\mathbf{v}_1|^2}{3}. \tag{3.8}$$

These conditions provide a system of 5 equations defined by (3.6), (3.7) and (3.8) in the 4 complex variables $\mathbf{w}_0, \mathbf{w}_1, \mathbf{v}_0, \mathbf{v}_1$ and 2 real variables $\alpha > 0, \gamma$. They can be recast as a system of 9 real equations in 10 real variables ($\alpha > 0, \gamma$, the real and imaginary parts of $\mathbf{w}_0, \mathbf{w}_1, \mathbf{v}_0, \mathbf{v}_1$). It should be noted that these equations are nonlinear, therefore the proof of the existence of solutions and their behavior with respect to the prescribed arc length are difficult to obtain.

Note the special structure of the first equation in (3.6), we choose a special case as

$$\mathbf{v}_0 = \sqrt{\alpha}\mathbf{w}_1$$

to analyze the solution. Substituting in equations (3.6), (3.7) and (3.8), the conditions change

into

$$\begin{cases} \mathbf{v}_0 = \sqrt{\alpha}\mathbf{w}_1, \\ \sqrt{\alpha}\mathbf{v}_1 = \gamma\mathbf{w}_1 - \alpha^2\mathbf{w}_0, \\ \mathbf{w}_0^2 + \mathbf{w}_0\mathbf{w}_1 + \mathbf{w}_1^2 = 3(P_3 - P_0), \\ \alpha^3\mathbf{w}_0^2 - (\alpha^2 + 2\gamma\alpha)\mathbf{w}_0\mathbf{w}_1 + (\alpha + \gamma + \gamma^2\alpha^{-1})\mathbf{w}_1^2 = 3(Q_3 - P_3), \\ (1 + \alpha^3)|\mathbf{w}_0|^2 + (1 - \alpha^2 - 2\alpha\gamma)\text{Re}(\overline{\mathbf{w}}_0\mathbf{w}_1) + (1 + \alpha + \gamma + \gamma^2\alpha^{-1})|\mathbf{w}_1|^2 = 3l. \end{cases} \tag{3.9}$$

Transforming the third and fourth equation in (3.9), we can get

$$\begin{cases} (\alpha^3 + \alpha^2 + 2\gamma\alpha)\mathbf{w}_0^2 = 3(\alpha^2 + 2\gamma\alpha)(P_3 - P_0) + 3(Q_3 - P_3) - (\alpha^2 + \alpha + 2\gamma\alpha + \gamma + \gamma^2\alpha^{-1})\mathbf{w}_1^2, \\ (\alpha^3 + \alpha^2 + 2\gamma\alpha)\mathbf{w}_0\mathbf{w}_1 = 3\alpha^3(P_3 - P_0) - 3(Q_3 - P_3) - (\alpha^3 - \alpha - \gamma - \gamma^2\alpha^{-1})\mathbf{w}_1^2, \end{cases}$$

Divide the two equations, the conditions (3.9) finally turn into

$$\begin{cases} \mathbf{v}_0 = \sqrt{\alpha}\mathbf{w}_1, \\ \sqrt{\alpha}\mathbf{v}_1 = \gamma\mathbf{w}_1 - \alpha^2\mathbf{w}_0, \\ \mathbf{w}_0 = \frac{3(\alpha^2 + 2\gamma\alpha)(P_3 - P_0) + 3(Q_3 - P_3) - (\alpha^2 + \alpha + 2\gamma\alpha + \gamma + \gamma^2\alpha^{-1})\mathbf{w}_1^2}{3\alpha^3(P_3 - P_0) - 3(Q_3 - P_3) - (\alpha^3 - \alpha - \gamma - \gamma^2\alpha^{-1})\mathbf{w}_1^2}\mathbf{w}_1, \\ (\alpha^3 + \alpha^2 + 2\gamma\alpha)\mathbf{w}_0^2 = 3(\alpha^2 + 2\gamma\alpha)(P_3 - P_0) + 3(Q_3 - P_3) - (\alpha^2 + \alpha + 2\gamma\alpha + \gamma + \gamma^2\alpha^{-1})\mathbf{w}_1^2, \\ (1 + \alpha^3)|\mathbf{w}_0|^2 + (1 - \alpha^2 - 2\alpha\gamma)\text{Re}(\overline{\mathbf{w}}_0\mathbf{w}_1) + (1 + \alpha + \gamma + \gamma^2\alpha^{-1})|\mathbf{w}_1|^2 = 3l, \end{cases} \tag{3.10}$$

Clearly, the variables $\mathbf{v}_0, \mathbf{v}_1, \mathbf{w}_0$ can be considered as functions of $\mathbf{w}_1, \alpha, \gamma$, therefore we just need to solve the variables $\mathbf{w}_1, \alpha, \gamma$ through the last two equations in (3.10).

Obviously, under the special assumption $\mathbf{v}_0 = \sqrt{\alpha}\mathbf{w}_1$ by complex representation, the problem finally turns into 3 real equations in 4 real variables ($\alpha > 0, \gamma$, the real and imaginary part of \mathbf{w}_1). It seems that the calculation of the problem is simplified. However, the 3 equations are still complicated nonlinear equations and explicit solutions are still difficult to obtain.

3.4. Computation

Since our construction involves the solution of a set of nonlinear equations with coefficients dependent on the specified data, the existence of such interpolants in all instances is non-obvious. However, using the same ideas and methods in [5, 6], the thorough analyses in these two references assure the solvability of our problem. Moreover, because of the nonlinear nature of the equations, explicit symbolic solution is very difficult to be found. Therefore, we transform the above nonlinear equations problem into the following equivalent constrained-optimization problem (3.11). So the G^2 blending problem changes into an optimization problem with nonlinear constraints.

The following presented examples are all performed using the interior-point algorithm of the ‘fmincon’ constrained-optimization function in MATLAB. The efficiency of the method is enhanced by exploiting the fact that the constraints have simple and closed-form expressions.

All of the calculations are carried out on a PC with 8 GHz cpu.

$$\begin{aligned}
 \min \quad & F = u_0^2 + v_0^2 + u_0u_1 + v_0v_1 + u_1^2 + v_1^2 + s_0^2 + t_0^2 + s_0s_1 + t_0t_1 + s_1^2 + t_1^2 \\
 \text{s.t.} \quad & \begin{cases} \alpha > 0, \\ \alpha u_1v_1 - s_0t_0 = 0, \\ \alpha(u_1^2 - v_1^2) - s_0^2 + t_0^2 = 0, \\ u_0^2 + u_0u_1 + u_1^2 - v_0^2 - v_0v_1 - v_1^2 + 3x_0 - 3x_3 = 0, \\ 2(u_0v_0 + u_1v_1) + u_0v_1 + u_1v_0 + 3y_0 - 3y_3 = 0, \\ s_0^2 + s_0s_1 + s_1^2 - t_0^2 - t_0t_1 - t_1^2 + 3x_3 - 3x_4 = 0, \\ 2(s_0t_0 + s_1t_1) + s_0t_1 + s_1t_0 + 3y_3 - 3y_4 = 0, \\ (\alpha + \gamma)(u_1^2 - v_1^2) - \alpha^2(u_0u_1 - v_0v_1) - s_0^2 + t_0^2 - s_0s_1 + t_0t_1 = 0, \\ 2(\alpha + \gamma)(u_1v_1) - \alpha^2(u_0v_1 + u_1v_0) - 2s_0t_0 - s_0t_1 - s_1t_0 = 0, \\ u_0^2 + v_0^2 + u_0u_1 + v_0v_1 + u_1^2 + v_1^2 + s_0^2 + t_0^2 + s_0s_1 + t_0t_1 + s_1^2 + t_1^2 \geq 3l. \end{cases} \quad (3.11)
 \end{aligned}$$

4. Examples

In this section, we list some examples to illustrate our method in operation.

Example 4.1 Suppose that the given points and total arc length are

$$P_0 = (-2, -3), \quad P_3 = Q_0 = (0, 10), \quad Q_3 = (3, 4), \quad l = 30.8612$$

respectively. Since the solution is not unique, the ‘good’ solution can be identified as the one with the least value for the absolute rotation index defined by

$$R = \int_0^1 |\kappa(\xi)|\sigma(\xi)d\xi,$$

which has closed-form evaluation, as described in [17]. In this case, the original problem changes into a minimization problem with constraint conditions (3.5). For this example, the ‘good’ solution is

$$\begin{aligned}
 \overline{\Lambda}_{11} &= [u_0, u_1, v_0, v_1, s_0, s_1, t_0, t_1, \alpha, \gamma] \\
 &= [-2.1618, -3.4467, -3.3259, -1.4529, -4.6167, -1.4067, -1.9461, \\
 &\quad 5.2094, 1.7941, 2.5655],
 \end{aligned}$$

and the resulting control points are

$$\begin{aligned}
 P_0 &= (-2.0000, -3.00000), \quad P_1 = (-4.1294, 1.7933), \\
 P_2 &= (-3.2565, 6.6614), \quad P_3 = (-1.7771e - 04, 9.9998), \\
 Q_1 &= (5.8420, 15.9896), \quad Q_2 = (11.3861, 8.8853), \\
 Q_3 &= (2.9998, 4.0000),
 \end{aligned}$$

with the interpolant shown in Figure 1(a), while the solution corresponding to the values

$$\overline{\Lambda}_{12} = [u_0, u_1, v_0, v_1, s_0, s_1, t_0, t_1, \alpha, \gamma]$$

$$=[1.6867, 5.0856, 6.0308, -1.0132, 3.5352, 0.9029, -0.7044, -2.3186, 0.4832, 0.2009]$$

and the resulting control points

$$\begin{aligned} P_0 &= (-3.0000, -4.00000), & P_1 &= (-13.1752, 3.7814), \\ P_2 &= (-8.2791, 13.4352), & P_3 &= (-1.8352e - 04, 10.0000), \\ Q_1 &= (4.0003, 8.3399), & Q_2 &= (4.5199, 5.3957), \\ Q_3 &= (2.9996, 4.0000). \end{aligned}$$

is still a correct formal solution for the same data, shown in Figure 1 (b). It can be easily checked that these two solutions are just the special case discussed in Section 3.3 as in (3.10).

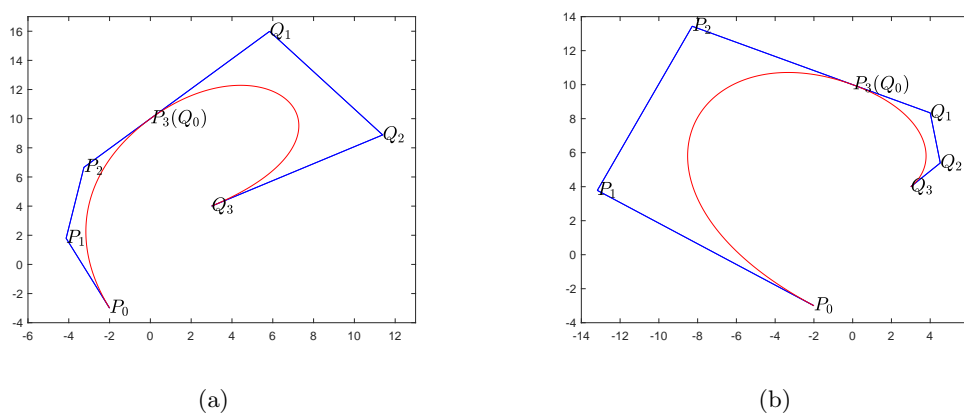


Figure 1 Two solutions for Example 4.1

For fixed points $P_0, P_3(Q_0), Q_3$, the next example illustrates the behavior of interpolants with increasing arc length l .

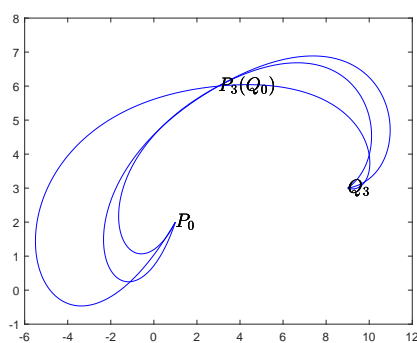


Figure 2 Interpolants for Example 4.2 with increasing arc lengths $l = 20.1803, 24.1803$ and 28.1803 , respectively

Example 4.2 For the control points

$$P_0 = (1, 2), P_3 = Q_0 = (3, 6), Q_3 = (9, 3),$$

Figure 2 illustrates the solutions for the sequence of increasing total arc lengths l as 20.1803, 24.1803 and 28.1803, respectively.

Example 4.3 Note that the given three control points in both of the above two examples all form convex broken lines, in this example we consider given control points

$$P_0 = (0, 0), P_3 = Q_0 = (5, -8), Q_3 = (9, 2),$$

distributed as a concave broken line. Figure 3 (a) shows two interpolating cubic PH curves with prescribed total arc length $l_{31} = 20.9604, l_{32} = 22.2043$, respectively, while Figure 3 (b) presents two solutions to the interpolation problem with prescribed arc length $l_{33} = 31.2043$.

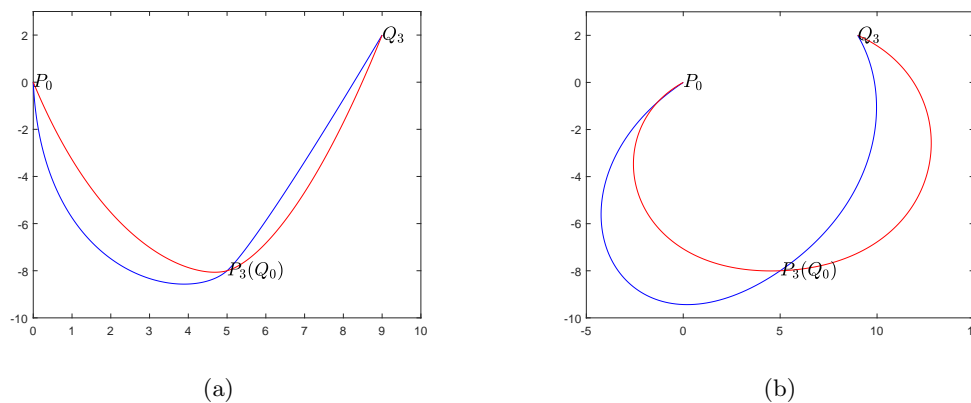


Figure 3 The solution obtained by different arc length of Example 4.3

Remark 4.4 Quintic or even the higher degree planar PH Bézier curve can also be used to solve the above interpolation problem, while by quintic PH Bézier curve we can obtain two G^3 blending curves with prescribed total arc length.

5. Conclusions

In free-form curve design, interpolation of boundary data with a prescribed arc length may be desired to satisfy certain geometrical or physical constraints. Taking advantage of the distinctive properties of PH curves, the problem of constructing two cubic planar PH curves with given end points P_0, Q_3 and G^2 continuous blending at joint point $P_3(Q_0)$ with specified total arc length l is discussed herein. Exploiting the PH curve representation in control points and the G^2 blending condition, the problem finally turns into an optimization problem with nonlinear constraints. Moreover, very simple and efficient solutions can be easily obtained. Furthermore, by construction, the computed interpolants are found to be convex or concave curve when the given control points are distributed as convex or concave broken line.

By appealing to the excellent characteristics of PH curves, this study is only a basic investigation into the possibility of geometric blending. It accommodates an efficient solution that admits a very straightforward implementation. There are several interesting directions in which the present results may possibly be extended, including:

- interpolation of higher-order local data, such as end curvatures;
- the interpolation from planar data to spatial data;
- the imposition of global shape measures, such as the bending energy;
- geometric blending with prescribed segment arc length.

However, these are analytically and computationally more challenging problems, which are unlikely to possess simple and exact solutions as obtained in the present context.

Acknowledgements We thank the referees for their time and comments.

References

- [1] R. T. FAROUKI, T. SAKKALIS. *Pythagorean hodographs*. IBM J. Res. Dev., 1990, **34**(5): 736–752.
- [2] Y. TSAI, R. T. FAROUKI, B. FELDMAN. *Performance analysis of CNC interpolators for time-dependent feed rates along PH curves*. Comput. Aided Geom. Design, 2001, **18**(3): 245–265.
- [3] R. T. FAROUKI. *Pythagorean-Hodograph Curves: Algebra and Geometry Inseparable*. Berlin, Springer, 2008.
- [4] J. KOSINKA, M. LAVICKA. *Pythagorean hodograph curves: a survey of recent advances*. J. Geom. Graph., 2014, **18**(1): 23–43.
- [5] R. T. FAROUKI. *Construction of G^1 planar Hermite interpolants with prescribed arc lengths*. Comput. Aided Geom. Design, 2016, **46**: 64–75.
- [6] R. T. FAROUKI. *Existence of Pythagorean-hodograph quintic interpolants to spatial G^1 Hermite data with prescribed arc lengths*. J. Symb. Comput., 2019, **95**: 202–216.
- [7] M. HUARD, R. T. FAROUKI, N. SPRYNSKI, et al. *C^2 interpolation of spatial data subject to arc-length constraints using Pythagorean-hodograph quintic splines*. Graph Models, 2014, **76**: 30–42.
- [8] M. KRAJNC. *Interpolation with spatial rational Pythagorean-hodograph curves of class 4*. Comput. Aided Geom. Design, 2017, **56**: 16–34.
- [9] B. BASTL, M. BIZZARRI, K. FERJANCIC, et al. *C^2 Hermite interpolation by Pythagorean-hodograph quintic triarcs*. Comput. Aided Geom. Design, 2014, **31**(7-8): 412–426.
- [10] Z. HABIB, M. SAKAI. *G^2 Pythagorean hodograph quintic transition between two circles with shape control*. Comput. Aided Geom. Design, 2007, **24**(5): 252–266.
- [11] D. J. WALTON, D. S. MEEK. *G^2 curve design with a pair of Pythagorean hodograph quintic spiral segments*. Comput. Aided Geom. Design, 2007, **24**(5): 267–285.
- [12] Buqing SU, Dingyuan LIU. *Computational Geometry*. Science and Technology Press of Shanghai, Shanghai, 1981.
- [13] D. DAVID, N. SPRYNSKI. *Method and device for acquisition of a geometric shape*. Patent No. wo/2006/095109, 2006.
- [14] M. HUARD, N. SPRYNSKI, N. SZAFRAN, et al. *Reconstruction of quasi developable surfaces from ribbon curves*. Numer. Algorithms, 2013, **63**(3): 483–506.
- [15] Weijun ZHOU, Zhang LI. *A modified Broyden-like quasi-Newton method for nonlinear equations*. J. Comput. Appl. Math., 2020, **372**: 112744, 10 pp.
- [16] Gonglin YUAN, Shengwei YAO. *A BFGS algorithm for solving symmetric nonlinear equations*. Optimization, 2013, **62**(1): 85–99.
- [17] Bohan DONG, R. T. FAROUKI. *PH quintic: a library of basic functions for the construction and analysis of planar quintic Pythagorean-hodograph curves*. ACM Trans Math Soft, 2015, **41**(4), Article 28.